AD-A152 297 FAILURE PROCESSES IN PENETRATORS WITH SHEAR-CONTROL GROOVES(U) NAVAL WEAPONS CENTER CHINA LAKE CA S A FINNEGAN ET AL. NOV 84 NWC-TP-6542 SBI-AD-E900 427 1/1

UNCLASSIFIED F/G 19/1 NL

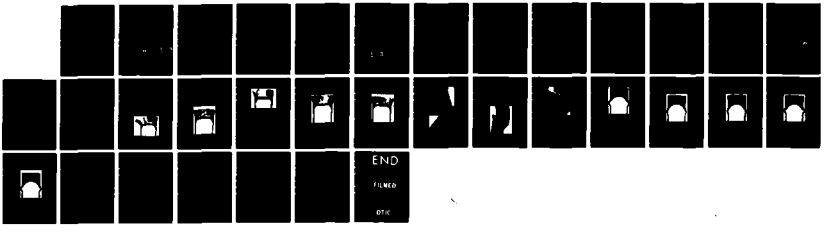

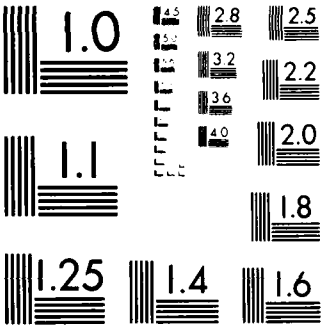

MICROCOPY RESOLUTION TEST CHART
NATIONAL BUREAU OF STANDARDS 1963-A

REPRODUCED AT GOVERNMENT EXPENSE

NWC TP 6542

(2)

AD-A152 297

Failure Processes in Penetrators With Shear-Control Grooves

by
Stephen A. Finnegan
and
John Pearson
Research Department

NOVEMBER 1984

NAVAL WEAPONS CENTER
CHINA LAKE, CA 93555-6001

DTIC
ELECTE
APR 1 1 1985
S D
B

DTIC FILE COPY

Approved for public release; distribution unlimited.

85 04 10 033

REPRODUCED AT GOVERNMENT EXPENSE

Naval Weapons Center

AN ACTIVITY OF THE NAVAL MATERIAL COMMAND

FOREWORD

This experimental study examines the failure processes in steel projectiles under target impact. This work was performed during Fiscal Years 1983 and 1984.

This effort was supported by the Naval Air Systems Command (NAVAIR) and was executed by the Naval Weapons Center (NWC) under the Surface/Aerospace Weaponry Technology Block Program. Funds to support the program were provided under AirTask A32-320J/008B/4F32-300-000 (Appropriation 1741319.41AJ). This airtask provides for continued exploratory development in the air-to-air and air-to-surface technology areas. Mr. H. Benefiel, AIR-320E, is the cognizant NAVAIR technology administrator, and Mr. L. N. Gilbert is the NWC technology manager for the warheads portion of the Block Program.

This report has been reviewed for technical accuracy by Marvin Backman, Research Department.

Approved by
E. B. ROYCE, *Head*
Research Department
November 1984

Under authority of
K. A. DICKERSON
Capt., U.S. Navy
Commander

Released for publication by
B. W. HAYS
Technical Director

NWC Technical Publication 6542

Published by ..... Technical Information Department
Collation ..... Cover, 15 leaves
First printing ..... 165 copies

UNCLASSIFIED

SECURITY CLASSIFICATION OF THIS PAGE (When Data Entered)

REPORT DOCUMENTATION PAGE

READ INSTRUCTIONS BEFORE COMPLETING FORM

1 REPORT NUMBER: NWC TP 6542	2. GOVT ACCESSION NO.: AD-A152-247
3. RECIPIENT'S CATALOG NUMBER:	
4 TITLE (and Subtitle): FAILURE PROCESSES IN PENETRATORS WITH SHEAR CONTROL GROOVES	5. TYPE OF REPORT & PERIOD COVERED:
	6. PERFORMING ORG. REPORT NUMBER:
7 AUTHOR(s): Stephen A. Finnegan and John Pearson	8. CONTRACT OR GRANT NUMBER(s):
9 PERFORMING ORGANIZATION NAME AND ADDRESS: Naval Weapons Center, China Lake, CA 93555-6001	10. PROGRAM ELEMENT, PROJECT, TASK AREA & WORK UNIT NUMBERS: AirTask A32-320J/008B/4F32-300-000
11 CONTROLLING OFFICE NAME AND ADDRESS: Naval Weapons Center, China Lake, CA 93555-6001	12. REPORT DATE: November 1984
	13. NUMBER OF PAGES: 28
14 MONITORING AGENCY NAME & ADDRESS (if different from Controlling Office):	15. SECURITY CLASS. (of this report): UNCLASSIFIED
	15a. DECLASSIFICATION DOWNGRADING SCHEDULE:

16 DISTRIBUTION STATEMENT (of this Report)

Approved for public release; distribution unlimited.

17 DISTRIBUTION STATEMENT (of the abstract entered in Block 20, if different from Report)

18 SUPPLEMENTARY NOTES

19 KEY WORDS (Continue on reverse side if necessary and identify by block number)

Penetrator
Warhead
Shear Control
Impact
Adiabatic Shear
Spall
Concrete

20 ABSTRACT (Continue on reverse side if necessary and identify by block number)

See back of form.

DD FORM 1 JAN 73 1473 EDITION OF 1 NOV 65 IS OBSOLETE

S/N 0102-LF-014-6601

UNCLASSIFIED

SECURITY CLASSIFICATION OF THIS PAGE (When Data Entered)

(U) *Failure Processes in Penetrators With Shear-Control Grooves* (U), by Stephen A. Finnegan and John Pearson. China Lake, Calif., Naval Weapons Center, November 1984. 28 pp. (NWC TP 6542, publication UNCLASSIFIED.)

(U) Metallographic studies were conducted on small, cylindrical steel projectiles, containing internal circumferential grooves, that had previously impacted thin steel or simulated concrete targets. These experiments were performed to examine the survivability, during impact, of penetrator warheads that used the shear-control method of fragmentation control. Projectiles tested against simulated concrete targets experienced outward bulging and eventually failure at higher impact speeds. Such failure normally occurred in the sidewall immediately behind its junction with the nose. Placement of a shear-control groove in this zone resulted in premature shear failure. Projectiles tested against thin steel targets typically failed by disintegration of the nose through a combination of (1) longitudinal fracturing associated with mushrooming of the frontal portion, (2) circumferential fracturing resulting from multiple spalling along the back surface, and (3) adiabatic shearing along the periphery of the impact surface. Sidewall bulging was less extensive than that experienced during impact against concrete for the same initial impact speed. However, the presence of a shear-control groove in this region resulted in the initiation of adiabatic shearing at the root of the groove.

CONTENTS

DTIC
ELECTE
APR 11 1986
B

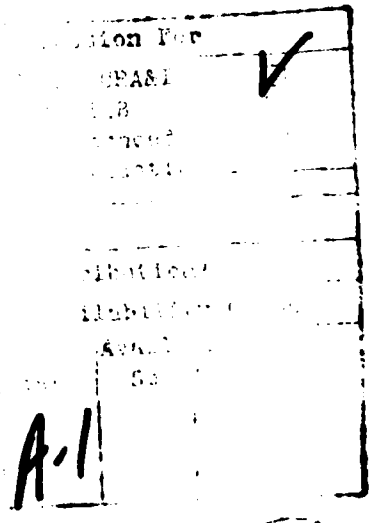

INTRODUCTION

The shear-control method of fragmentation control is now widely used in bombs and warheads to produce fragments of desired shapes and sizes and to achieve specific fragmentation signatures for weapons. First developed at the Naval Weapons Center (NWC), the technique uses a pattern of grooves which forms a grid system on the inner surface of the warhead case (References 1 and 2). This grid functions as a family of dynamic stress raisers and controls the locations of shear fracture initiation in the case during the detonation and case expansion process.

This control method is most effective in a warhead with case thickness and material properties such that shear fracture predominates in the fragmentation process. Good control also requires that the geometry of the grid pattern complements the strain-field geometry during case expansion and that the grid spacing and grid profile configurations are optimized for the required fragmentation signature.

This control method has been effectively used in a wide range of bomb and warhead sizes with a variety of different steels ranging from the lower-strength, plain, low-carbon types to many of the more ductile, high-strength, heat-treatable ones (Reference 1). To date, most of these applications have been for either air-burst or surface-burst weapons. However, there is also a need for fragmentation control methods suitable for the warheads of penetrator weapons to be used against hard and moderately hard targets. Accordingly, the shear-control method is currently being studied for possible use in penetrator weapons that will be employed against more resistant targets such as ships or reinforced concrete/earth structures. To be effective in these situations, the weapon must penetrate some distance into the target before the warhead is detonated. Since the warhead itself is the main penetrator component of the weapon, it must be designed to withstand severe loading conditions during the impact and penetration process. However, since a shear-control grid which has been machined or formed into the inner surface of the case may act as a stress raiser during target interaction, there has been concern that the presence of such a grid might affect the structural integrity of the case and, hence, the survivability of the weapon.

This report deals with part of an ongoing program designed to study this potential problem of grid usage and, if possible, to establish design limitations for the use of such grids. Experimental portions of this program involved the use of small-scale, steel penetrators which were gun-fired against targets of steel plate and targets of simulated concrete. The present report deals primarily with metallographic observations regarding the failure processes which occurred in these small-scale steel penetrators. One of the failure processes observed in these studies, and stressed in

this report, is the occurrence of concentrated shear bands in the microstructure of the steel which can serve as precursors to shear fracture.

BACKGROUND

A simple penetrator warhead consists basically of an explosive-filled, hollow, steel cylinder with a thick, solid nose section at the front (impact) end to protect the explosive filler and aid in the target penetration process. The front end of the penetrator is usually shaped in some manner to optimize penetration.

Damage to the penetrator as a result of target impact tends to occur in the nose section and at the junction between the nose and the cavity wall. For those penetrators with a relatively flat front, damage to the front end results initially from transient stress wave interactions which may cause spalling and corner fracturing if the stress pulses are sufficiently large in amplitude and of short duration, as are normally produced in the perforation of a steel plate target (Reference 3). As the transient effects die out, contact forces result in material flow along and away from the frontal surface. A different type of behavior (i.e., a typical mushroom shape) can result if the nose is sufficiently blunt, the material is ductile, and the contact forces acting on it are both large and of extended duration, as would be encountered in the penetration of a massive concrete target. These same forces also produce an outward bulging of the cavity wall at its junction with the nose. This zone of bulging is frequently referred to as the primary zone of failure, and it is within this region that failure of the wall normally occurs. It was originally thought that the presence of a shear-control grid on the inner surface of the penetrator wall might lead to premature failure of the wall during impact if placed sufficiently close to, or within, this primary zone of failure.

In order to investigate the effects of shear-control grids on the survivability of penetrator warheads, a series of small-scale tests were conducted against both simulated concrete and thin steel targets using gun-launched hollow steel penetrators containing a single circumferential groove on the inside surface of the cavity wall. This groove was located either within or behind the primary zone of failure, and its depth was varied for different tests. A number of smooth-wall penetrators (containing no internal groove) of the same size were also tested for comparison. In a complementary study, impact conditions were modeled analytically using a two-dimensional finite element code. In addition, a microstructural analysis, using reflected-light microscopy, was conducted on selected penetrators in order to study the damage process more intimately. The present report treats the results of the microstructural studies, although a brief description of the experimental procedures is also presented for completeness. The results of the experimental program and the analytical studies have been reported previously (References 4 and 5).

EXPERIMENTAL PROCEDURES

PENETRATORS

Penetrators consisted of 2-inch-long, 0.5-inch-diameter, flat-fronted, hollow steel cylinders machined from SAE 4340 steel bar stock. The nose of the penetrator was 0.25 inch thick in the center, and the cavity wall was 0.04 inch thick. The inside surface of the impact end was machined to a hemispherical shape in order to minimize stress concentrations that would ordinarily occur at the transition between nose and cavity wall during impact. Penetrators requiring a shear control groove contained a single circumferential "vee" groove with a 60-degree included angle and a depth of either 0.004 or 0.008 inch machined into the inside surface of the cavity wall. The circumferential groove was positioned either 0.46 or 0.71 inch from the front of the penetrator. A 0.46-inch distance placed the groove exactly at the junction between the nose and wall and in the primary zone of failure, while a 0.71-inch distance located the groove behind the expected zone of failure. After being machined, penetrators were heat-treated to a hardness of 38 40 R_C, after which the outside surface was plated with a thin (about 0.001-inch) coating of copper in order to minimize damage to the gun barrel during launching. The different penetrator designs used in these studies are shown in Figure 1. The relative overall behavior of the different designs has been described previously (Reference 4).

TARGETS

Penetrators were tested against two types of targets: thin steel and simulated concrete. Steel targets consisted of hot-rolled, 1 16-inch-thick, low-carbon sheet material with a hardness of 55 R_B. Simulated concrete targets were made of Thorite (Standard Dry Wall Products), a fast setting commercial concrete patching compound. The preparation of the Thorite targets has been described previously (Reference 4).

TEST PROCEDURE

Penetrators were impacted at normal incidence to the targets using a smooth-bore, 0.50 caliber evacuated powder gun. Targets were positioned sufficiently close to the gun muzzle (6 18 inches) so that impact velocities could be approximated by the values measured in the gun barrel. These velocities were obtained using a photo-diode system and a time-interval counter. A recovery trough filled with Celotex slabs was placed immediately behind the steel targets to capture any perforating penetrators. Impact velocities were varied from about 2000 ft s to about 3600 ft s. A more complete description of the experimental apparatus used has been documented previously (Reference 6).

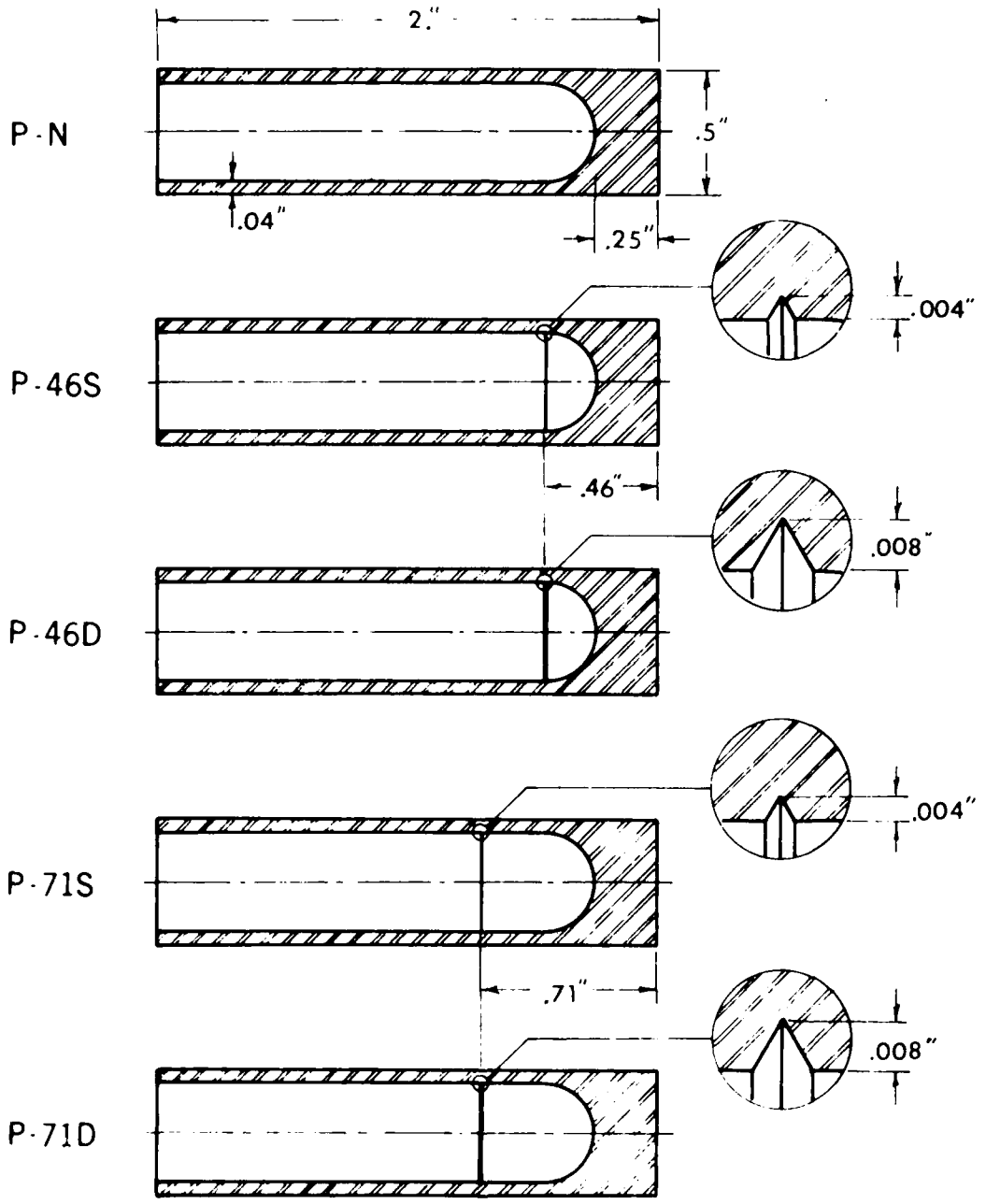

FIGURE 1. Cross-Sectional Views of Test Projectiles with Details of Grooves.

METALLOGRAPHIC PROCEDURE

Post-impact penetrators were cut in half lengthwise using a high-speed, water-cooled, cut-off wheel, after which the exposed half-sections were ground flat to a 15-micron finish and photographed. The forward portions of each section were then mounted in Bakelite and prepared, using standard metallographic techniques, for study with an optical microscope.

The primary microstructure of the hardened penetrator material consisted of fine tempered martensite with an average hardness of 39 R_C. In addition, bands of impurities (principally sulfides and oxides) were aligned along the long axis. Alignment of impurities occurs as a result of metal-working processes used in the manufacture of the material. This normally causes some reduction of strength in directions normal to the alignment direction.

GENERAL ANALYSIS OF PENETRATOR BEHAVIOR

The nature and degree of damage are determined by the target type, the impact velocity, the presence or absence of shear grooves, and, if shear grooves are present, the locations and depths of the grooves. Projectiles impacted against simulated concrete targets were subjected to relatively long-duration, moderate levels of stress which produced, at impact velocities above 2000 ft/s, a pronounced outward bulging of the cavity wall immediately behind its junction with the nose. At a velocity between 2100 and 2500 ft/s (the value depending on the presence or absence of a circumferential groove in the bulged zone and on the depth of the groove), shear fractures initiated in the bulged zone with, as a result, partial or complete severing of the nose portion from the wall. During the perforation of steel targets in the same impact velocity range, projectiles experienced very short duration, high stress levels with, as a result, a much smaller amount of bulging in the cavity wall. The reduction in sidewall damage was offset, however, by extensive damage to the nose of the penetrator in the form of multiple spalling and numerous fractures in the axial direction (Reference 7).

Metallographic examination of penetrators fired against both types of targets indicated that the formation of concentrated shear bands in the microstructure of the steel played a contributory role in the failure processes. For penetrators fired against steel targets, the shear bands appeared both in the surface area of the nose and in the bulged areas, being associated with shear fractures in both areas. The shear bands identified in these projectiles were of the white-etching, transformation type. For penetrators fired against Thorite targets, broad regions of deformation were found in some of the bulged areas, with what appeared to be the start of concentrated shear bands within those zones. However, examples of the fully formed, narrow, white-etching bands were not found in the limited number of specimens examined.

This process of shear failure in the bulged zones of the projectile sidewalls appears to be as follows. During the bulging and deformation of the sidewall in the

primary zone of failure, broad, indistinctly appearing regions of deformation approximately 0.01 inch wide are first formed. With continuing load the white-etching, narrow, concentrated bands of shear are then formed within these broad regions of deformation. Almost immediately following the formation of the narrow shear bands, shear fractures propagate through these bands and result in separation of the sidewall. Careful examination of shear fractures in the sidewall of the projectile frequently shows residual traces of the shear band along the edge of the fracture surface. Because of the identification of shear banding in the failure processes of the penetrators, a brief review is presented regarding the nature, formation, and geometrical orientation of such bands, followed by a brief discussion of the role they can play in certain types of ordnance applications.

SHEAR BANDS

NATURE AND FORMATION

Numerous ordnance materials, including many types of steels, uranium-based alloys, titanium alloys, and aluminum alloys, show evidence that, when they are subjected to intense loads of short duration, failure by shear fracture is often preceded by the formation of narrow bands of concentrated shear deformation in the microstructure of the material. The subsequent pattern of shear fracture may then be governed by the nature and geometry of the family of shear bands so produced.

Shear bands appear in two basic forms: "transformation" bands, which normally appear as narrow light-colored, etch-resistant zones within which the material has undergone a permanent phase transformation (as in many of the high-strength, heat-treatable steels), and "deformation" bands which appear as narrow zones of intense grain deformation (as in the plain, low-carbon steels). The "transformation" bands tend to be quite narrow with a width of up to about 20 μm, while the "deformation" bands are somewhat wider, being normally from one to several grain diameters wide. While the boundaries of a transformation band are usually well defined, deformation bands have relatively ill-defined boundaries owing to the gradual increase of deformation in the grain structure as the center of the band is approached. Perhaps the easiest way to establish the width of a deformation band is by means of a microhardness traverse.

Both types of shear bands are best observed by means of optical microscopy. Figures 2 and 3 show shear bands found in fragments from explosively loaded cylinders with shear-control grids. In both figures the shear band emanates from the root of a control groove element. Figure 2 shows a "transformation" type band as it appears in a higher strength steel (SAE 4340). A partial shear fracture is visible in the band. Figure 3 shows a typical "deformation" type band as it appears in a plain, low-carbon steel (SAE 1045). Both types of shear bands, which represent paths of reduced shear strength, then become the trajectories for the propagation of shear fracture through the metal.

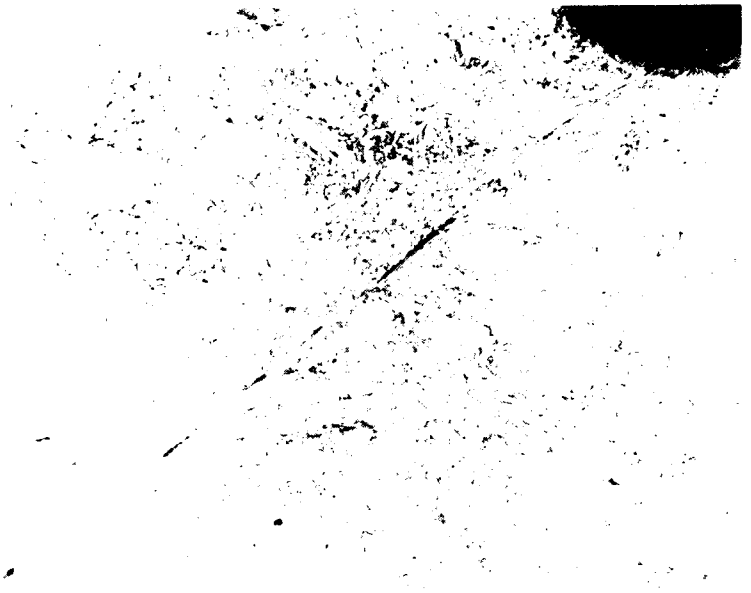

FIGURE 2. Photomicrograph of a Concentrated Shear Band in a Fragment from an Explosively Loaded SAE 4340 Steel Cylinder with a Shear-Control Grid (100X Magnification).

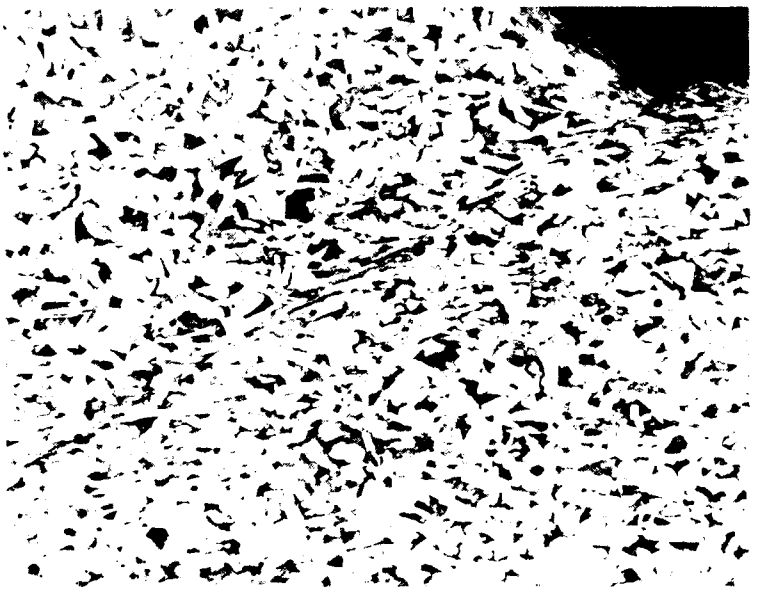

FIGURE 3. Photomicrograph of a Concentrated Shear Band in a Fragment from an Explosively Loaded SAE 1015 Steel Cylinder with a Shear Control Grid (100X Magnification).

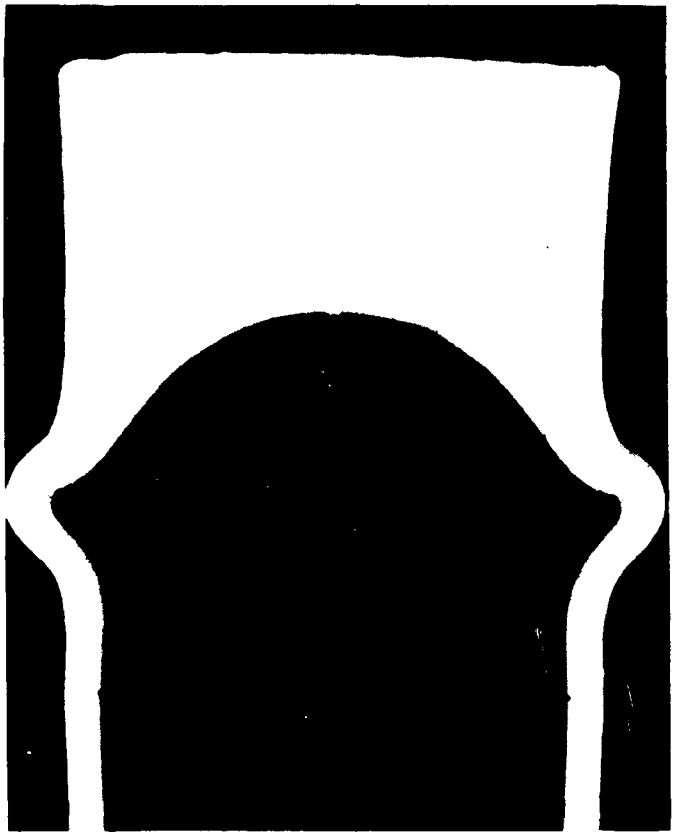

FIGURE 16. Section-View of Penetrator With Shallow Control Groove Behind Primary Failure Zone (P-71S) After Impact on Concrete Target at 2460 ft/s.

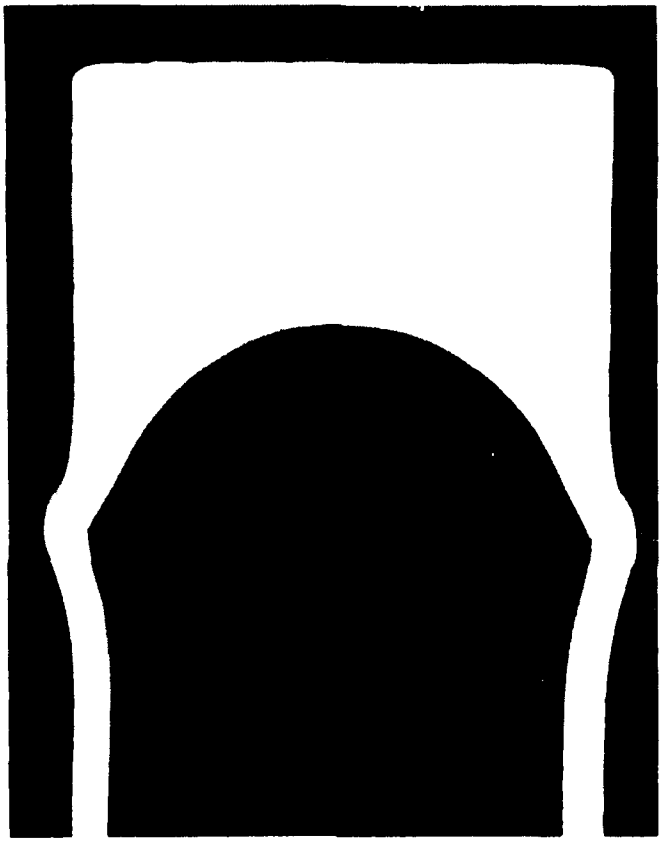

FIGURE 15 Section View of Penetrator With Deep Control Groove in Primary Failure Zone (P 46D) After Impact on Concrete Target at 2130 ft/s.

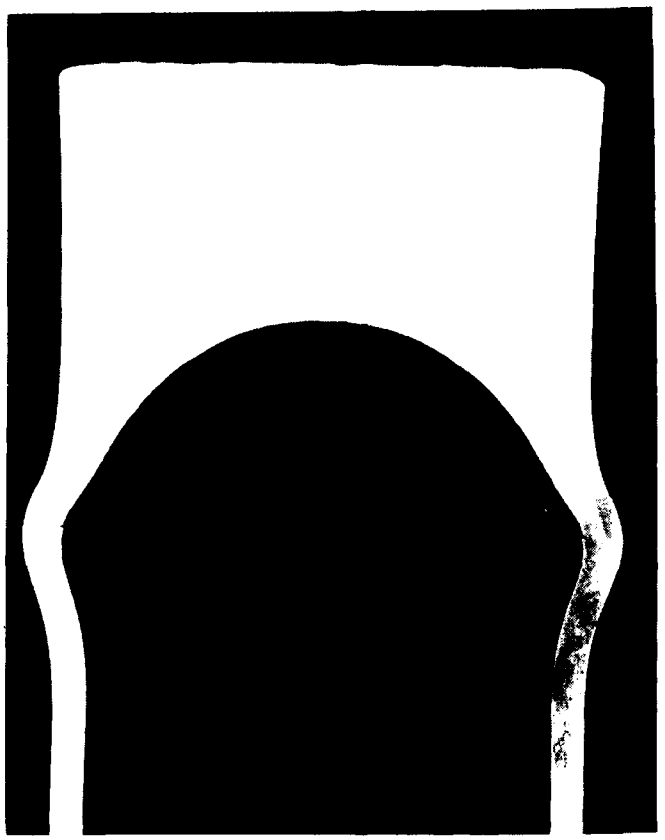

FIGURE 14. Section-View of Penetrator With Shallow Control Groove in Primary Failure Zone (P-46S) After Impact on Concrete Target at 2320 ft/s.

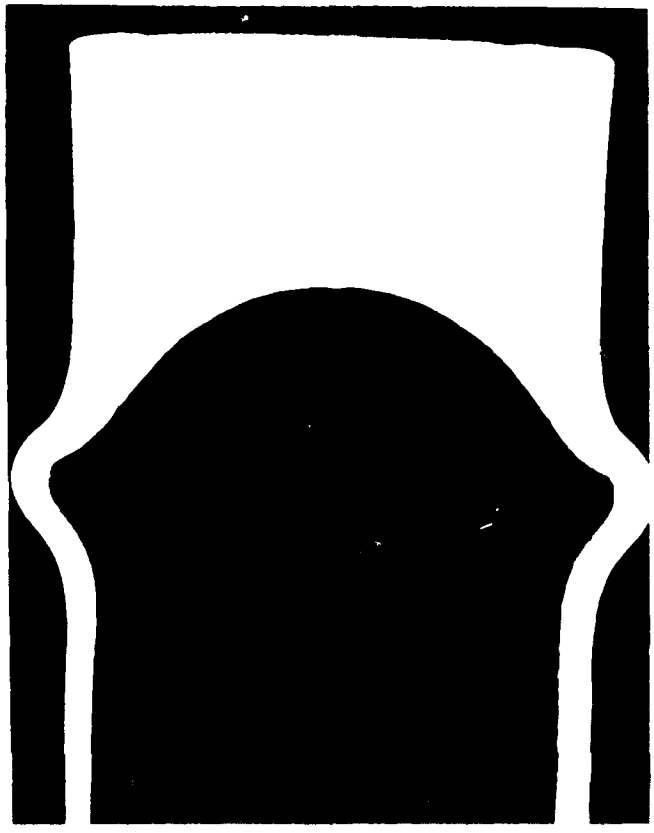

FIGURE 13. Section View of Smooth Wall Penetrator (F-N) After Impact on Concrete Target at 2490 ft/s.

The effect of [illegible] on the primary zone of failure can be seen in Figures 14 and [illegible] show the forward ends of penetrators that impacted at 2,320 and [illegible] respectively. Both penetrators had grooves located 0.46 inch from the [illegible] penetrator of Figure 14 had a shallow groove, while the [illegible] had a deep groove.

Figures 16 and [illegible] the control groove at a distance of 0.71 inch from [illegible] penetrator shown in Figure 16 had a shallow groove at impact [illegible] The penetrator shown in Figure 17 had a deep groove at impact [illegible] Control grooves placed at this location had little effect on side-[illegible] the massive bulging and, at higher impact velocities, complete [illegible] all occurred in the primary zone of failure.

FIGURE 12. Photomicrograph of Concentrated Shear Bands in Incipient Shear Failure Zone Shown in Figure 11 (75X magnification).

BEHAVIOR AGAINST SIMULATED CONCRETE TARGETS

Small-scale penetrators, with and without shear-control grooves, were fired at simulated concrete targets. At impact speeds of about 2200 ft/s and above, smooth wall penetrators showed a significant amount of outward bulging in the cavity wall at its junction with the nose. This effect can be seen in Figure 13, which shows the forward end of a plain-wall penetrator which impacted at 2490 ft/s. While noticeable bulging of the sidewall occurred, no fractures were formed.

For penetrators impacting at a slightly higher velocity, about 2500 ft/s, complete shear failure of the wall occurred on the forward edge of the bulged zone, and the nose section was squeezed backward into the inside of the bulged portion of the cavity wall. At increasing impact speeds this process caused the cavity wall to split open longitudinally in several places, with the individual wall segments forming outward-curling petals.

Figure 11 shows a control groove as it appears in the bulged region of a penetrator which impacted at 2830 ft/s. This projectile had a deep control groove located 0.46 inch from the front surface. The groove was almost closed during the deformation of the sidewall. A white shear band can be seen extending from the region of the groove to the outside surface of the sidewall. Figure 12 shows an enlarged view of the shear band. It appears that several zones of incipient shear fracture have formed within the band. The propagation and linking together of such fractures along the entire length of the shear band would ultimately produce catastrophic failure and separation by complete shear fracture through the wall of the penetrator. This type of shear-band associated failure in the sidewall of a projectile can be seen in Figure 6. This projectile, which had a deep control groove located 0.46 inch from the front surface, failed in the sidewall at an impact velocity of 2950 ft/s. Microstructural examination showed that the shear fracture in the sidewall had propagated through a precursor band of concentrated shear in the microstructure of the steel.

FIGURE 11. Photomicrograph of Incipient Shear Failure in a Primary Failure Zone Containing a Deep Control Groove (P 46D) After Impact on a Steel Target at 2830 ft/s (50X magnification)

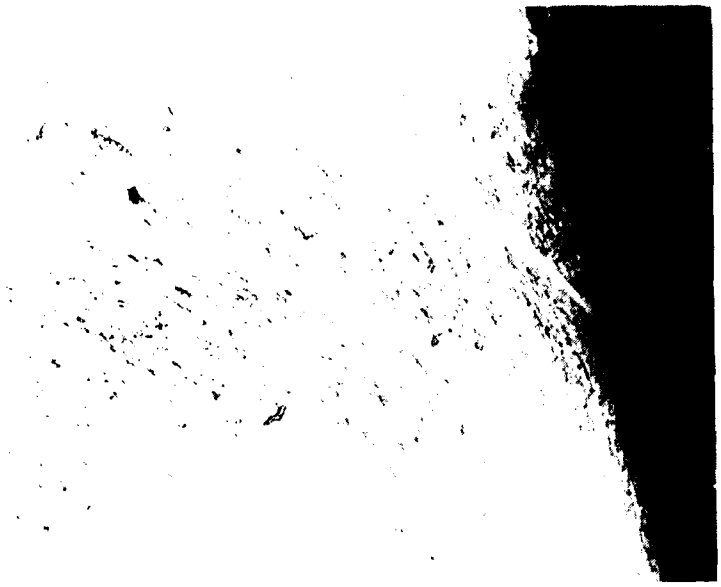

FIGURE 9. Photomicrograph of Concentrated Shear Bands at Outer Edge of Front Surface in Penetrator Shown in Figure 7 (200X magnification).

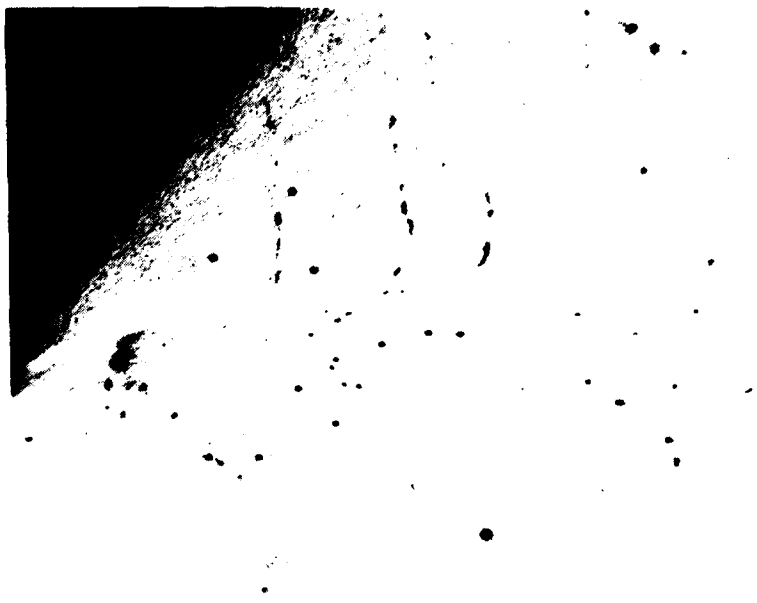

FIGURE 10. Photomicrograph of Concentrated Shear Band at Outer Edge of Front Surface in Penetrator Shown in Figure 7 (200X magnification).

FIGURE 8. Section-View of Penetrator With Deep Control Groove Behind Primary Failure Zone (P-71D) After Impact on Steel Target at 2970 ft/s.

FIGURE 7. Section View of Penetrator With Shallow Control Groove Behind Primary Failure Zone (P-71S) After Impact on Steel Target at 2980 ft/s.

FIGURE 6. Section-View of Penetrator With Deep Control Groove in Primary Failure Zone (P-46D) After Impact *on Steel Target at 2950 ft/s.*

Figures 7 and 8 show penetrators which impacted at similar velocities of 2980 and 2970 ft/s, respectively. Both penetrators had grooves located 0.71 inch from the front end of the projectile and outside of the primary zone of failure. The penetrator of Figure 7 had a shallow groove, while the penetrator of Figure 8 had a deep groove. Although the buckling was somewhat greater for the deep groove, neither of these penetrators sustained shear fractures in the sidewall. As all of these figures show, the primary mode of failure for the penetrators which impacted thin steel targets was disintegration of the nose and not failure of the sidewall.

White-etching shear bands were identified both in the surface areas of the nose and in the bulged areas of the sidewalls. In both locations the shear bands were associated with the formation of shear fractures. Figures 9 and 10 are representative of the concentrated shear bands which formed along the outer edge of the projectile face. Figure 9 shows multiple bands as they appeared in a projectile which impacted at 2980 ft/s, while Figure 10 shows a single band formed on the opposite side of the same projectile (see Figure 7).

In addition to the damage sustained by the nose section, buckling occurred in the sidewall, mainly in the region just behind the nose section. The degree of buckling produced depended on the impact velocity and on the depth and location of the circular groove, if one were present. Figures 5 and 6 show this sidewall effect for penetrators which impacted at similar velocities of 2985 and 2950 ft/s, respectively. Both penetrators had grooves located 0.46 inch from the front end of the projectile so that the grooves were located in the primary zone of failure. The penetrator of Figure 5 had a shallow groove which resulted in minor buckling not much different from that sustained by the plain wall penetrator of Figure 4 at about the same impact velocity. The penetrator shown in Figure 6 had a deep groove which resulted in complete failure of the sidewall due to shear fracture emanating from the groove.

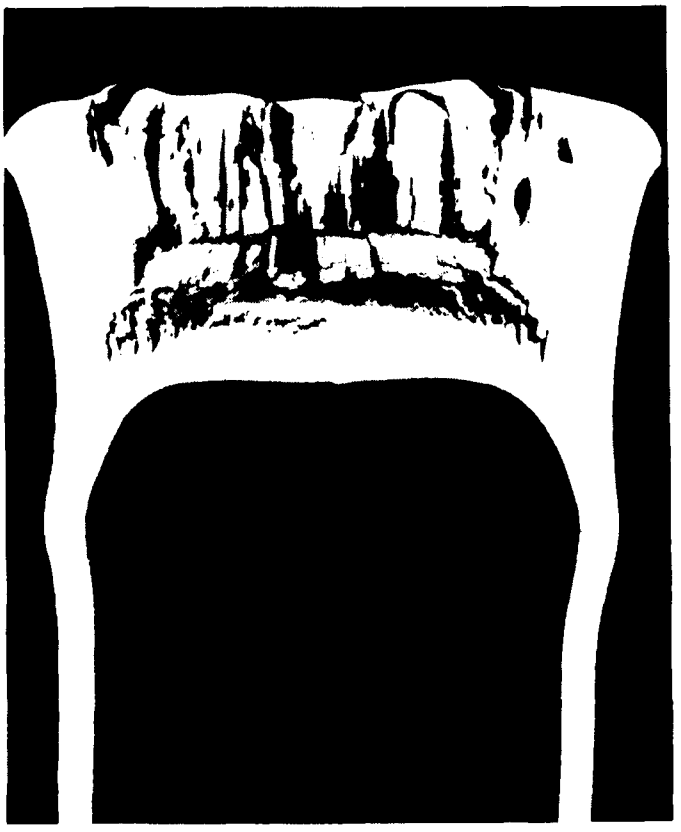

FIGURE 5. Section-View of Penetrator With Shallow Control Groove in Primary Failure Zone (P-46S) After Impact on Steel Target at 2985 ft/s.

extremely short impact durations which caused extensive stress wave interactions in the penetrator nose.

Penetrators without grooves were tested at impact speeds up to about 3600 ft/s without incurring failure by fracture in the sidewall, even though at the higher speeds the nose was nearly completely destroyed. Penetrators with grooves located in the primary zone of failure showed shear fractures emanating from some of the deep grooves at the higher impact velocities, but the primary modes of failure again occurred in the nose sections of the penetrators.

Figure 4, which is an axial cross section of the forward portion of a plain-wall penetrator (no grooves) which impacted at 2995 ft/s, shows the various failure patterns encountered. Nose damage includes (1) lateral bulging of the frontal portion accompanied by axially oriented tensile fractures, some of which radiate outward from the center of the nose and others of which appear as circular ring fractures, with both geometries occasionally terminating with a shear lip at the frontal surface; (2) shear bands along the outside edge of the frontal surface; and (3) a family of parallel tensile fracture surfaces identified as spall fractures, which resulted from stress wave reflections off the back surface of the nose. As many as five spall surfaces were found at the higher impact speeds, a process requiring very high-amplitude, short-duration stress transients.

FIGURE 4. Section-View of Smooth-Wall (P-N) Penetrator After Impact on Steel Target at 2995 ft/s.

and projected unchanged to the condition of fracture. Among these are (1) the orientation of the principal stresses, (2) the principal plane of tensile failure, and (3) the geometrical pattern of the maximum shear trajectories. This approach provides a relatively simple means by which the geometrical orientation of the preferred planes of shear failure can be predicted even under the intense loads produced by high velocity impact or contact detonation. It is along these preferred planes of shear failure that the shear bands are formed, becoming in many instances the pathways for shear fracture. Of major importance in this approach is the fact that, in the behavioral comparison between the statically and impulsively loaded systems, the geometrical pattern of the maximum shear trajectories remains the same whether the metal is in the elastic or the fully yielded condition (Reference 12).

ROLE IN ORDNANCE APPLICATIONS

In ordnance applications shear bands have been studied mainly in terms of the failure processes of metal targets subjected to projectile impact (References 9, 13, and 14). To a lesser degree they have been studied for the role they may play in the fragmentation process of explosively loaded cylinders or fragmentation warheads (References 15 and 16). Pearson and Finnegan have also related the formation of concentrated shear bands to the highly effective fragmentation control exercised by shear-control grids (Reference 16). Other investigators have discussed the possible role of shear bands in the shatter behavior of kinetic energy penetrators and related the penetration performance of different penetrator materials, at least in part, to their relative tendency to shear adiabatically at the impact surface (Reference 17).

While a thorough understanding of shear banding is still lacking in terms of required stress intensities, time rates of loading, the thermomechanical processes of formation, and other physical and metallurgical aspects of their behavior, the role of shear bands in ordnance applications is quite clear. In many instances they are the precursor to catastrophic failure by shear fracture. Fortunately, even though the overall knowledge of shear band formation and behavior is still quite limited it is possible, as indicated above, to predict the geometrical aspects of shear band formation and the subsequent pattern of shear fracture. This geometrical analysis can then be applied in order to (1) use these failure patterns to enhance the effectiveness of certain types of ordnance, such as controlled fragmentation warheads, or (2) restrict their formation through appropriate design, as in the survivability of targets or penetrators.

RESULTS

BEHAVIOR AGAINST THIN STEEL TARGETS

Penetrators which impacted thin steel targets suffered extensive damage to the nose in addition to cavity-wall damage. The type of damage sustained by the penetrator nose in this type of engagement resulted from the large contact forces and

The "transformation" type of shear bands was first described by Zener and Hollomon (Reference 8). They are commonly found in martensitic steels loaded at high strain rates. Described as "adiabatic shears" (Reference 8) or "concentrated shear bands" (Reference 9), they are generally thought to be thermally softened zones that initiate and grow along trajectories of maximum shear stress if the rate of heating within the zone from mechanical work exceeds the rate of dissipation by conduction processes. The etch-resistant white band is considered to be an untempered martensite which results if the temperature of the shear band becomes high enough to transform the iron into its high-temperature (austenite) phase; the surrounding metal thereupon serves as a massive heat sink and a high cooling rate results. Recently, Rogers and Shastry showed, with microhardness measurements, that the white-etching transformed band is usually preceded by a light-etching shear band showing intense deformation only (Reference 10).

That the "deformation" type of shear band performs the same failure function in other metals, that such deformations can be initiated by the same general intensities and geometries of load, and that the appearance difference is a function of material properties are more recently recognized phenomena. As Rogers has pointed out (Reference 11), the majority of the adiabatic shear observations reported in nonferrous metals are of the deformed type, while the transformed type is principally observed in ferrous metals (the plain, low-carbon steels are a notable exception).

GEOMETRIC ANALYSIS

In the geometric sense, shear bands follow the trajectories of maximum shear which exist in the metal part during the loading process. Thus, in predicting the potential orientation of shear bands in an impulsively loaded metal body, one must first establish the geometry of the stress field which is formed, and from that geometry determine the orientation of the trajectories of maximum shear. A general analysis requires that the dynamic behavior of the impulsively loaded metal be momentarily "frozen" so that the stress field that exists at any given instant in a particular element of the body can be viewed by static concepts. Even though the magnitudes of the loads and the time-histories of loading may be drastically different between the statically and impulsively loaded systems, the orientation of the principal stresses and the planes of maximum shear as they are momentarily established in the element of the body can be determined from static loading concepts (i.e., elastic theory). The shear plane that is most apt to support failure can also be readily determined from a three-dimensional Mohr's circle analysis based on the relative magnitudes of the three principal strains.

By not involving the actual quantitative values of stress, many of the complexities which occur in going from the elastic state through gross deformation and finally to fracture can be avoided. Rather, the analysis is restricted to certain qualitative and behavioral features which can be established from elastic relations

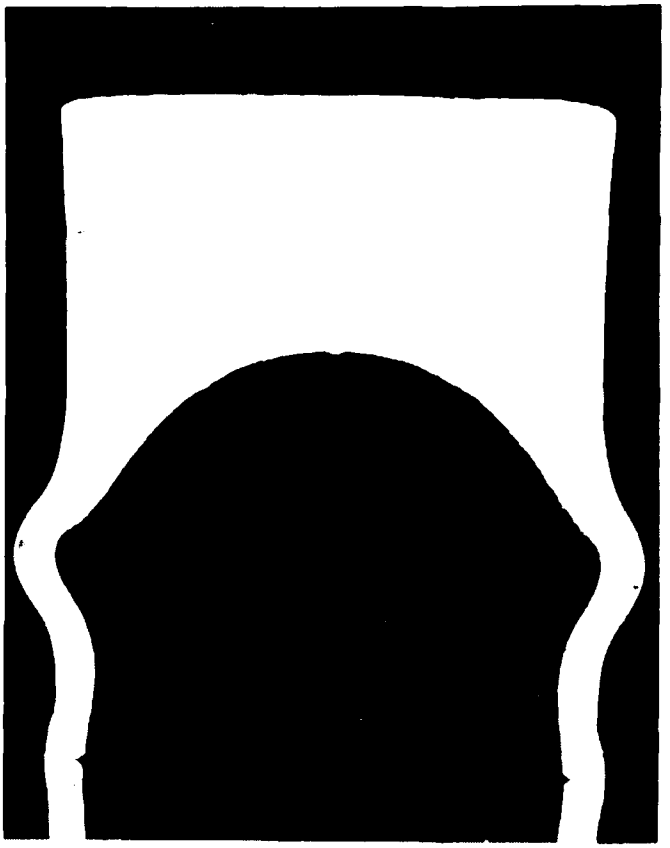

FIGURE 17. Section-View of Penetrator With Deep Control Groove Behind Primary Failure Zone (P-71D) After Impact on Concrete Target at 2448 ft/s.

When circumferential grooves were present in the heavily bulged areas, pairs of broad, rather difficult-to-see bands of deformation were frequently found, with the bands emanating at about 45 degrees from the region of the collapsed groove. It appears that the formation of these bands was related to the collapse process of the groove, since the locations of their inner and outer boundaries coincided with the closure length of the groove.

These broad bands of deformation were first noticed when polished and etched half-sections were viewed under oblique lighting conditions. Under a highly directional fiber-optic light beam, they showed up as either light or dark regions depending on the orientation of the sample with respect to the beam. When viewed under normally incident lighting the bands were difficult to see although some alignment of the grains was observed. In specimens that impacted the simulated concrete targets, the deformation band directed toward the nose of the projectile was generally more distinct, as though it had undergone a greater degree of deformation. When wall failure by shear fracture occurred, the fracture normally propagated through the band with this particular orientation. Deformation bands of this type were also sometimes associated with the lesser bulging which occurred when the grooves were located outside the primary failure zone. In such a situation, both of the deformation bands appeared to be of similar intensity. Complete failure of the wall was not observed at this location, although some permanent bulging was observed at the higher impact velocities, as shown in Figure 17.

REFERENCES

1. John Pearson. "The Shear-Control Method of Warhead Fragmentation," in *Proceedings of the Fourth International Symposium on Ballistics*. Naval Postgraduate School, Monterey CA, 17–19 October 1978. (Publication UNCLASSIFIED.)

2. Naval Weapons Center. *Parametric Studies for Fragmentation Warheads*, by John Pearson. China Lake, CA, NWC, April 1968. (NWC TM 4507, publication UNCLASSIFIED.)

3. John S. Rinehart and John Pearson. *Behavior of Metals Under Impulsive Loads*. Cleveland, The American Society for Metals, 1954.

4. Naval Weapons Center. *Survivability of Penetrators With Circumferential Shear-Control Grooves*, by J. C. Schulz and O. E. R. Heimdahl. China Lake, CA, NWC, April 1981. (NWC TP 6275, publication UNCLASSIFIED.)

5. ———. *Survivability Analysis for Impacting Warheads With Shear-Control Grids*, by O. E. R. Heimdahl and John Pearson. China Lake, CA, NWC, February 1982. (NWC TP 6288, publication UNCLASSIFIED.)

6. W. Goldsmith and S. A. Finnegan. "Penetration and Perforation Processes in Metal Targets At and Above Ballistic Velocities," *Intl. J. Mech. Sci.*, Vol. 13 (1971), pp. 843–866.

7. W. J. Stronge and J. C. Schulz. "Projectile Impact Damage Analysis," *J. Computers and Structures*, Vol. 13, No. 1–2 (1981), pp. 287–294.

8. C. Zener and J. H. Pollomon. "Effect of Strain Rate Upon Plastic Flow of Steel," *Journal of Applied Physics*, Vol. 15 (1944), pp. 22–32.

9. L. E. Samuels and I. R. Lamborn. "Failures of Armament Hardware," in *Metallography in Failure Analysis*, ed. by James L. McCall and P. M. French. New York, Plenum Press, 1978. Pp. 167–190.

10. H. C. Rogers and C. V. Shastry. "Material Factors in Adiabatic Shearing in Steels," in *Shock Waves and High-Strain-Rate Phenomena in Metals*, ed. by Marc A. Meyers and Lawrence E. Murr. New York, Plenum Press, 1980. Pp. 285–298.

11. H. C. Rogers. "Adiabatic Plastic Deformation," *Ann. Rev. Mater. Sci.*, Vol. 9 (1979), pp. 283-311.

12. F. K. Th Van Iterson. *Plasticity in Engineering*. New York, Hafner, 1947).

13. M. E. Backman and S. A. Finnegan. "The Propagation of Adiabatic Shear," in *Metallurgical Effects at High Strain Rates*, ed. by R. W. Rohde, et al. New York, Plenum Press, 1973. Pp. 531-543.

14. Y. Me-Bar and D. Shechtman. "On the Adiabatic Shear of Ti-6A1-4V Ballistic Targets," *Materials Science and Engineering*, Vol. 58 (1983), pp. 181–188.

15. J. C. Beetle, J. V. Rinnovatere, and J. D. Corrie. "Fracture Morphology of Explosively Loaded Steel Cylinders," in *Proc. Fourth Annual Scanning Electron Microscope Symposium*. Chicago, ITT Research Institute, April 1971, pp. 137 144. (Paper UNCLASSIFIED.)

16. J. Pearson and S. A. Finnegan. "A Study of the Material Failure Mechanisms in the Shear-Control Process," in *Shock Waves and High-Strain-Rate Phenomena in Metals*, ed. by Marc A Meyers and Lawrence E. Murr. New York, Plenum Press, 1980. Pp. 205-218.

17. G. J. Irwin. "Metallographic Interpretation of Impacted Ogive Penetrators." Valcartier, Canada, Defense Research Establishment, October 1972. (DREV-R-652/72, publication UNCLASSIFIED.)

INITIAL DISTRIBUTION

24 Naval Air Systems Command
- AIR-03 (1)
- AIR-03A (1)
- AIR-03B (1)
- AIR-03C (1)
- AIR-03D (1)
- AIR-310 (1)
- AIR-310B (2)
- AIR-320 (1)
- AIR-320A (1)
- AIR-320C (1)
- AIR-320E, H. Benefiel (1)
- AIR-320G, B. Sobers (1)
- AIR-320H, Dr. Habayeb (1)
- AIR-320K, D. Hutchins (1)
- AIR-330 (1)
- AIR-526 (1)
- AIR-530HD (1)
- AIR-536 (1)
- AIR-541 (1)
- AIR-5412 (1)
- AIR-7226 (2)
- PMA-242, Viars (1)

2 Chief of Naval Operations
- OP-506E (1)
- OP-982E (1)

7 Naval Sea Systems Command
- SEA-06A (1)
- SEA-62 (1)
- SEA-62R (1)
- SEA-62R41 (1)
- SEA-09B312 (2)
- PMS-4053 (1)

4 Chief of Naval Research, Arlington
- ONR-200 (1)
- ONR-260 (1)
- ONR-430 (1)
- ONR-432 (1)

1 Deputy Assistant Secretary of the Navy (Research and Advanced Technology)
1 Commander in Chief, U.S. Pacific Fleet (Code 325)
1 Commander, Third Fleet, Pearl Harbor
1 Commander, Seventh Fleet, San Francisco
2 David W. Taylor Naval Ship Research and Development Center, Bethesda
- Code 1606 (1)
- Code 166 (1)

2 Naval Academy, Annapolis (Director of Research)
1 Naval Air Development Center, Warminster (Code 60)

4 Naval Intelligence Support Center
  NISC 35 (1)
  NISC 36 (1)
  NISC 41 (1)
  NISC 42 (1)
3 Naval Postgraduate School, Monterey
  Aeronautical Engineering Department, A. Fuhs (1)
  Dean of Research (1)
  Mechanical Engineering (1)
3 Naval Ship Weapon Systems Engineering Station, Port Hueneme
  Code 5711, Repository (2)
  Code 5712 (1)
1 Naval Surface Weapons Center, Dahlgren (Code K21)
3 Naval Surface Weapons Center, White Oak Laboratory, Silver Spring
  K20 (1)
  K204 (1)
  R44 (1)
1 Naval War College, Newport
2 Office of Naval Technology, Arlington
  MAT-071 (1)
  MAT-0713, PEM, Surface-Aerospace Weaponry (1)
1 Pacific Missile Test Center, Point Mugu (Code 2200)
3 Army Missile Command, Redstone Arsenal
  DRDMI-TDK (2)
  DRSMI-RLA (1)
1 Air Force Systems Command, Andrews Air Force Base (AFSC/SD2)
1 Air Force Armament Division, Eglin Air Force Base (AD/XRP, L. Deidler)
1 Air Force Armament Division, Eglin Air Force Base (AFATL/DLJ)
1 Air Force Armament Division, Eglin Air Force Base (AFATL/DLJG)
1 Air Force Armament Division, Eglin Air Force Base (AFATL/DLM)
1 Air Force Armament Division, Eglin Air Force Base (AFATL/DLMA, C. B. Butler)
1 Air Force Armament Division, Eglin Air Force Base (AFATL/DLX)
1 Air Force Armament Division, Eglin Air Force Base (AFATL/DLY)
1 Air Force Intelligence Service, Bolling Air Force Base (AFIS/INTAW, Maj. R. Lecklider)
2 Air Force Wright Aeronautical Laboratories, Wright-Patterson Air Force Base (AFWAL/FIGC)
1 Air Force Wright Aeronautical Laboratories, Wright-Patterson Air Force Base (AFWAL/FIMG)
1 Deputy Under Secretary of Defense, Research and Advanced Technology (Engineering Technology)
1 Defense Advanced Research Projects Agency, Arlington (Strategic Technology Office)
12 Defense Technical Information Center
1 Langley Research Center (NASA), Hampton (Mail Stop 409)
1 Ford Aerospace and Communications Corporation, Ridgecrest, CA (R. J. Surprenant)
1 General Dynamics Corporation, Ridgecrest, CA (G. Myer)
1 Grumman Aerospace Corporation, Ridgecrest, CA (A. Duvall)
1 Hughes Aircraft Corporation, Ridgecrest, CA (T. Andress)
1 Martin Marietta Aerospace, Western Regional Office, El Segundo, CA (D. G. Somers)
1 Raytheon Manufacturing Company, Missile Systems Division, Bedford, MA
1 Raytheon Company, Ridgecrest, CA (M. Slater)
1 Rockwell International Corporation, Columbus, OH (Technical Information Center)
1 Rockwell International Corporation, El Segundo, CA (Technical Information Center)
1 Vought Corporation, Ridgecrest, CA (T. Ingram)

OFFICIAL BUSINESS PENALTY FOR PRIVATE USE, $300 GOVERNMENT

END

FILMED

5-85

DTIC